Biotransformation of Intestinal Bacterial Metabolites of Ginseng Saponin to Biologically Active Fatty-acid Conjugates

Hideo Hasegawa[1] and Ikuo Saiki[2]

[1]*Fermenta Herb Institute Inc., 1-30-15 Motohongo, Hachioji, Tokyo 192-0051, Japan*

[2]*Institute of Natural Medicine,*

Toyama Medical and Pharmaceutical University, 2630 Sugitani, Toyama 930-0194, Japan

Abstract

Ginsenosides are metabolized (deglycosylated) by intestinal bacteria to active forms after oral administration. 20(*S*)-Protopanaxadiol 20-*O*-β-D-glucopyranoside (M1) and 20(*S*)-protopanaxatriol (M4) are the main intestinal bacterial metabolites (IBMs) of protopanaxadiol- and protopanaxatriol-type glycosides. M1 was selectively accumulated into the liver soon after its intravenous (i.v.) administration to mice, and mostly excreted as bile; however, some M1 was transformed to fatty acid ester (EM1) in the liver. EM1 was isolated from rats in a recovery dose of approximately 24 mol%. Structural analysis indicated that EM1 comprised a family of fatty acid mono-esters of M1. Because EM1 was not excreted as bile as M1 was, it was accumulated in the liver longer than M1. The *in vitro* cytotoxicity of M1 was attenuated by fatty acid esterification, implying that esterification is a detoxification reaction. However, esterified M1 (EM1) inhibited the growth of B16 melanoma more than M1 *in vivo*. The *in vivo* antitumor activity paralleled with the pharmacokinetic behavior. In the case of M4, orally administered M4 was absorbed from the small intestine into the mesenteric lymphatics followed by the rapid esterification of M4 with fatty acids and its spreading to other organs in the body and excretion as bile. The administration of M4 prior to tumor injection abrogated the enhanced lung metastasis in the mice pretreated with 2-chloroadenosine more effectively than in those pretreated with anti-asialo GM1. Both EM1 and EM4 did not directly affect tumor growth *in vitro*, whereas EM1 promoted tumor cell lysis by lymphocytes, particularly non-adherent splenocytes, and EM4 stimulated splenic NK cells to become cytotoxic to tumor cells. Thus, the esterification of IBM with fatty acids potentiated the antitumor activity of parental IBM through delay of the clearance and through immunostimulation. These results suggest that the fatty acid conjugates of IBMs may be

the real active principles of ginsenosides in the body.

Introduction

Ginseng (the roots of *Panax ginseng* C. A. Meyer, Alariaceae) has been used as one of the most valuable traditional medicines in the Orient for over 2000 years. It contains a number of active constituents including saponins, essential oil, phytosterol, carbohydrates and sugars, organic acids, nitrogenous substances, amino acids and peptides, plus vitamins and minerals.[1,2] Pharmacological and clinical studies conducted over the past 40 years have focused on radioprotective, antitumor, antiviral and metabolic effects; antioxidant activities; nervous system and reproductive performance; effects on cholesterol and lipid metabolism, and endocrinological activity.[3,4] More recently, epidemiological studies have identified an association between ginseng intake and a decreased incidence and growth of cancers.[5-8]

The main ingredients of ginseng are ginsenosides, glycosides containing an aglycone (protopanaxadiol or protopanaxatriol) with a dammarane skeleton. So far, numerous researchers have contributed to the accumulation of evidence that ginsenosides are responsible for the pharmacological effects of ginseng; however some have obtained results from direct addition of ginsenoside into cell cultures *in vitro* or from intraperitoneal (i.p.) or intravenous (i.v.) injection to experimental animals, though ginseng is generally used as a drug taken orally. Pharmacokinetic studies have demonstrated that orally administered ginsenosides pass through the stomach and small intestine without decomposition by either gastric juice or liver enzymes into the large intestine, where ginsenosides are metabolized by colonic bacteria.[9] 20(*S*)-Protopanaxadiol 20-*O*-β-D-glucopyranoside, referred to as M1 or compound K, and 20(*S*)-protopanaxatriol (M4) are major intestinal bacterial metabolites (IBMs) of ginsenosides.[9] These metabolites mediate the anticancer actions of ginsenosides.[9] The IBMs are further esterified with fatty acid-conjugates (EM1 and EM4), which potentiated the activity of IBMs through effective accumulation in the body.[9-12] The major object of this article is to review the recent advance of studies on the biotransformation of IBMs to biologically active fatty acid-conjugates.

Biotrasformation of M1 to Its Fatty Acid Mono Esters

Pharmacokinetics of M1[10]

Immediately following a single i.v. injection of M1 (25 mg/kg), this metabolite disappeared

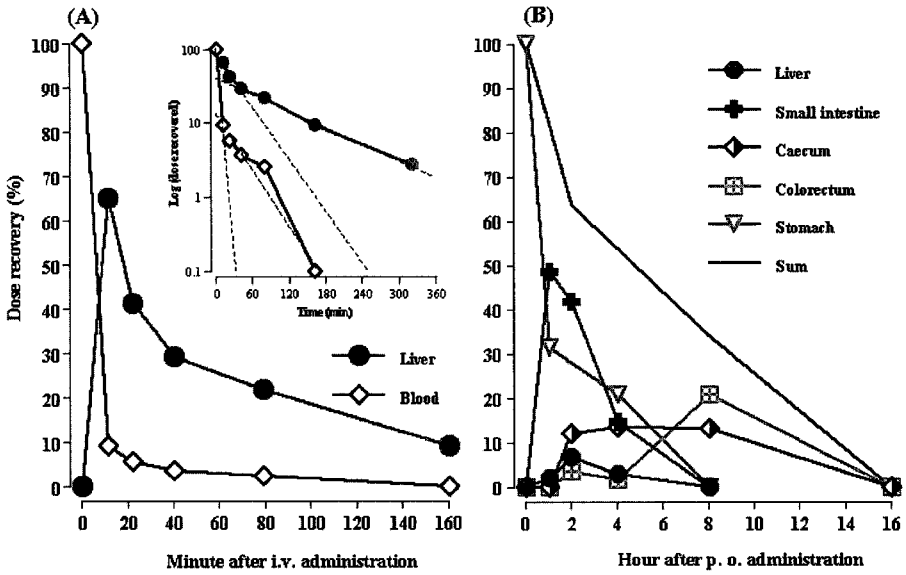

Fig. 1. Distribution of M1 after Administration to Mice.
M1 was dissolved in 8% Tween 20/PBS to make an injection at a concentration of 5 mg/ml (M1-Tw/PBS). Mice were given a single i.v. (**A**) or oral (**B**) administration of M1-Tw/PBS at a dose of 25 mg/kg (0.1 ml/20 g body weight). The mice were sacrificed at the indicated time after administration. Immediately following sacrifice of the animals, contents of the stomach, small intestine, caecum and colorectum were homogenized in saline (6 ml) and extracted twice with 40 ml of ethyl acetate (AcOEt). The AcOEt layer was evaporated to dryness and then dissolved in 0.5 ml of a methanol solution of *n*-butyl *p*-hydroxybenzoate (5 μg/ml) as an internal standard for HPLC analysis. The amounts of M1 in samples were determined by HPLC. Each point represents the mean value of % dose recovery from 2 to 3 animals.

from the blood ($t_{1/2\alpha}$, 3 min; $t_{1/2\beta}$, 23 min; *AUC*, 2815 minμg/ml), and instead increased in the liver. The level of M1 peaked at 10 min (C_{max}, 65% recovery) and thereafter gradually disappeared with time ($t_{1/2\alpha}$, 25 min; $t_{1/2\beta}$, 75 min; *AUC*, 481.4 hμg/g) (Fig. 1A). On the other hand, orally administered M1 was detected in the contents of the stomach, small intestine, caecum and colorectum with the passage of time (Fig. 1B), closely related to the movement of M1 in the gastrointestinal tract. Although M1 was undetectable in the blood (data not shown), it was detected in the liver, where it reached the maximal level (8% recovery) 2 h after administration and then gradually decreased (*AUC*, 115.5 hμg/g). Therefore, these results indicated that orally administered M1 was absorbed mainly from the small intestine into the blood followed by absorption from its accumulation in the liver.

To quantify M1 in organs, biological samples resected from mice 40 min after the i.v. injection

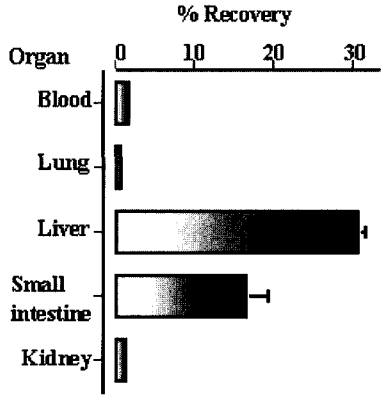

Fig. 2. Quantification of M1 in Organs after i. v. Injection.

(25 mg/kg) were analyzed by HPLC (Fig. 2). Much of the M1 was recovered from the liver and contents of the small intestine and a slight amount from the blood, lung and kidney (a total of 50% of the dose was recovered).

M1 (25 mg/kg) was administered i.v. to C57BL/6 mice. Forty min later, the mice were sacrificed and the lung, liver, kidny and contents of the small intestine were homogenized in saline (6 ml) and extracted twice with 40 ml of AcOEt. The AcOEt layer was evaporated to dryness and then dissolved in 0.5 ml of a methanol solution of *n*-butyl *p*-hydroxybenzoate (5 μg/ml) as an internal standard for HPLC analysis. The amounts of M1 in samples were determined by HPLC. Each bar represents the mean ± S.D. of % dose recovery from 3 animals.

Metabolism of M1 in the liver

To examine the metabolism of M1, the liver and contents of the small intestine from M1-treated mice were compared with those of untreated animals using TLC. A band, referred to as EM1, was newly detected 20 min after the i.v. injection of M1. Its color density peaked at 40 min, the turning point of the pharmacokinetic curve of M1 in the liver from α-phase to β -phase (Fig. 1A) and thereafter gradually decreased. At 160 min, the band of EM1 was still detectable, but not M1 (Fig. 3A). EM1 was also detected in the liver together with M1 after the oral administration of the latter (Fig. 3C). EM1 was hardly detected in the small intestine tissue; however, M1 was slightly detected (data not shown). In contrast with the liver, neither the band of EM1 nor any other new band except for M1 was detected in the contents of the small intestine (Fig. 3B), indicating that neither EM1 nor its metabolites except M1 was excreted as bile.

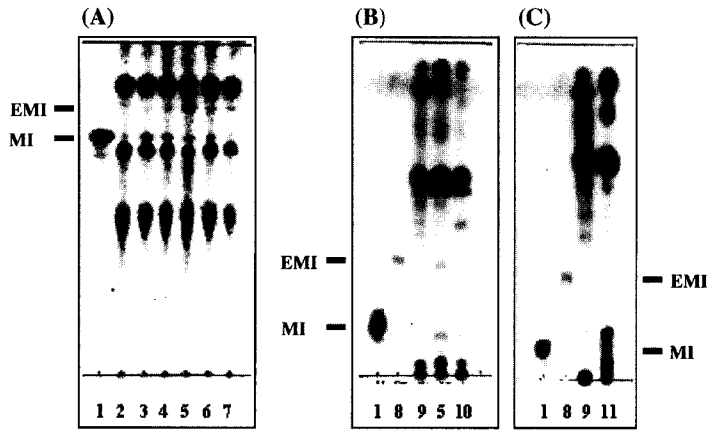

Fig. 3. TLC Profiles of M1-metabolites in the Liver.
C57BL/6 mice were given a single i.v. (**A** and **B**) or oral (**C**) administration of M1 (25 mg/kg). At the indicated time after administration, biological samples from the livers and contents of the small intestine were analyzed by TLC: TLC plate, silica gel 70 F_{254}; developing solvent, $CHCl_3$-MeOH-H_2O (65 : 35 : 10 v/v, lower phase) (**A**) or $CHCl_3$-EtOH (8 : 1 v/v) (**B** and **C**). Plates were stained by spraying with 8% vanillin-MeOH/72% H_2SO_4 (1: 5, v/v) followed by heating at 140 °C for 3 min. (**1**) M1, (**2**) recovery of 60 μg M1, (**3-7**) the livers treated with M1 (i.v.) (**3**, 10 min; **4**, 20 min; **5**, 40 min; **6**, 80 min; **7**, 160 min), (**8**) a mixture of chemically synthesized stearate and oleate (1: 1) of M1, (**9**) the liver of untreated control, (**10**) the contents of the small intestine at 40 min after i.v. M1-treatment and (**11**) the liver at 2 h after oral M1-treatment.

To examine whether the metabolism of M1 can include variation of aglycone structure or conjugation with acids such as glucuronic and sulfuric acids or with other cellular or tissue components, the liver resected from 40 min after i.v. injection of M1 was divided into three equal parts: one part was untreated control and the others were treated with alkaline or β-glucuronidase, followed by TLC and HPLC analyses. Although both M1 and EM1 were detected in the untreated control, no products except them were newly detected in the samples treated with either alkaline or β-glucuronidase. The amounts of M1 increased in the alkaline-treated sample compared to the untreated control, however. These results showed that M1 was mainly metabolized to esters without structural variation.

Structural Elucidation of EM1

For structural elucidation of EM1, it was isolated from the liver of rats administered with M1 (i.v.). Although EM1 was likely to be a single compound on normal phase TLC plates (Fig. 3), two bands (*Rf*, 0.14 and 0.18) were detected on reverse phase TLC plates. Moreover, EM1 was

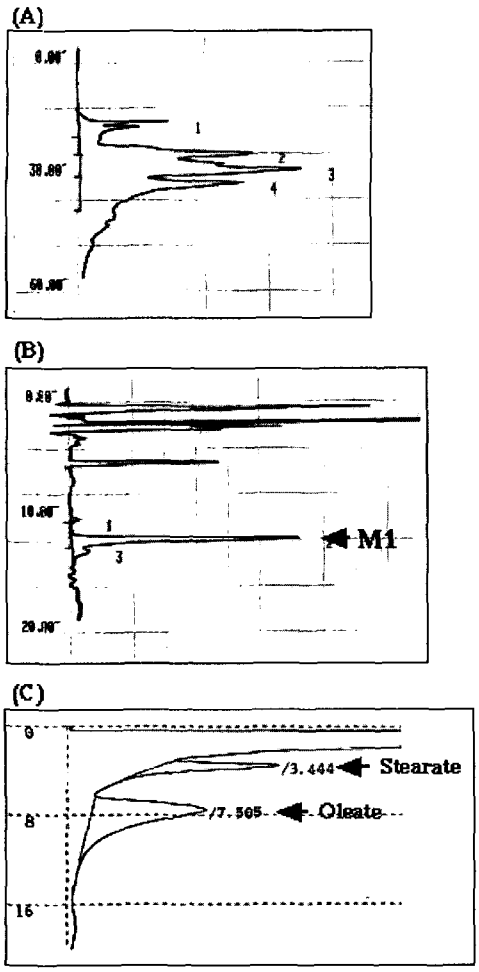

Fig. 4. Structural elucidation of EM1.
EM1 was analyzed by HPLC (**A**) followed by basic hydrolysis or transesterification. The amounts of M1 or fatty acids contained in EM1 were separately determined by HPLC (**B**) or GC (**C**).

For structural elucidation, EM1 was isolated as follows: M1, which was dissolved in Tw/PBS, was injected (4 ml, including 20 mg M1) into the tail vein of two Wistar male rats under light pentobarbital anesthesia. Two hours later, the livers (22.2 g) were resected, homogenized in 100 ml of ice-cooled saturated aqueous $NaHCO_3$ and extracted twice with 500 ml of AcOEt. The AcOEt layer was washed with saturated aqueous $NaHCO_3$ (200 ml) and water (200 ml), and then evaporated to dryness (673 mg). The oily residue was dissolved in 1 ml of $CHCl_3$, injected into a Sep-Pak Plus cartridge (Long Body Silica), washed with 12 ml of $CHCl_3$ and eluted with 12 ml of $CHCl_3$-EtOH (16 : 1, v/v) which was collected by 2-ml fraction. The fractions containing EM1 and M1, checked using TLC (normal phase), were individually evaporated *in vacuo* to afford crude EM1 (6.7 mg, 24 mol% dose recovery) and M1 (6.0 mg, 30 mol% dose recovery). Further, the crude EM1 was dissolved in 1 ml of 90% MeOH, injected to a Sep-Pak Original cartridge (C_{18}, Waters), washed with 12 ml of the same solvent and eluted with 12 ml of 100% MeOH. The fractions containing EM1 were evaporated *in vacuo* to give EM1 (2.8 mg). A part of EM1 was dissolved in MeOH to make a concentration of 1 mg/ml (EM1-MeOH).

A: EM1 was analyzed by HPLC (column, IPG-ODS, 8-10 μm, 4.6 i.d.×150 mm; solvent, 100% MeOH; detection, UV 215 nm; column temperature, 40°C; flow rate, 0.1 ml/min).

B: M1 contained in EM1 was measured following basic hydrolysis and the content determined by HPLC. Briefly, 0.1 ml of 0.5 mg/ml EM1-MeOH was reacted with 0.1 ml of 10% NaOH-MeOH at room temperature. Three hours later, 1 ml of water was added to the reaction mixture and the whole was extracted with 0.5 ml of water-saturated *n*-BuOH. An aliquot of the *n*-BuOH layer (20 μl) was then analyzed by HPLC (column, LiChroCART 250-4 LiChrospher 100 RP-18, 5 μm 4 i. d.×250 mm, Merck, Darmstadt, Germany; solvent, CH_3CN -H_2O, 55:45, v/v; detection, UV 203 nm; column temperature, 25°C; flow rate, 1.0 ml/min).

C: Fatty acids contained in EM1 were measured following transesterification and the content determined by GC. Briefly, 0.1 ml of 0.5 mg/ml EM1-MeOH was added to 0.1 ml of 6% HCl -MeOH and the mixture was heated at 60°C for 3 h. In parallel, fatty acids were also esterified as standards for GC analysis. After being cooled, 0.4 ml of saturated aqueous $NaHCO_3$ was added to the reaction mixture and the whole was extracted with 0.2 ml of AcOEt. An aliquot of the AcOEt layer (10 μl) was then analyzed by GC (column, DEGS 2% Uniport HPS 80/100 glass column 2.6 i. d.×2 m; column temperature, 160°C; carrier gas, N_2 65 ml/min). The identification and quantification were made by comparison of the *Rt* values and area of GC data with those of standard fatty acids.

For the standard of fatty acid esters of M1, it was esterified with fatty acids using the Schotten-Baumann method. Briefly, 5 mg (8 μmol) of M1 was dissolved in 1 ml of AcOEt and mixed with 1 ml of saturated aqueous $NaHCO_3$. Fatty acyl chloride (160 μmol) was added under ice-cooling and the mixture was stirred at room temperature overnight. An aliquot of the AcOEt layer (2 μl) was analyzed by TLC. The esters of M1 with stearic acid or oleic acid showed the same *Rf* values of 0.33 on silica gel 70 F_{254} plates ($CHCl_3$-EtOH, 8 : 1 v/v) but different *Rf* values on RP-8 F_{254S} plates (stearate 0.14, oleate 0.18; 100% MeOH).

determined by reverse phase HPLC to be a mixture of at least four compounds (Fig. 4A); however, its hydrolysis by alkaline produced M1 alone (Fig. 4B). This implied that EM1 comprised a family of M1 esters. Because the liver is rich in fatty acids, fatty acid esters of M1 were synthesized. Each fatty acid ester of M1 was detected as doublet-like peaks by reversed phase HPLC, suggesting that it was a mixture of structural isomers. The *Rf* and t_R values of EM1 were consistent with those of synthesized mono-esters of stearic and oleic acids, but with neither di- nor tri-esters (data not shown). In addition, GC analysis indicated that fatty acids contained in EM1 were mainly stearic and oleic acids (Fig. 4C).

To examine the components of EM1 in detail, we analyzed the metabolite by mass spectrometry. Low resolution FAB MS of EM1 in the presence of added NaCl produced strong ions at *m/z* 911, 909 and 883 corresponding to the pseudomolecular ions $[C_{54}H_{96}O_9$ (stearate) + $Na]^+$, $[C_{54}H_{94}O_9$ (oleate) + $Na]^+$ and $[C_{52}H_{92}O_9$ (palmitate) + $Na]^+$. Furthermore, high resolution FAB MS for EM1 gave ions *m/z* 911.6942 ($C_{54}H_{96}O_9Na$, $[M + Na]^+$; theoretical *m/z* 911.6953), 909.6774 ($C_{54}H_{94}O_9Na$, $[M + Na]^+$; theoretical *m/z* 909.6796) and 883.6596 ($C_{52}H_{92}O_9Na$, $[M + Na]^+$; theoretical *m/z* 883.6639). However, the data on low resolution FAB MS of EM1 also showed weak ions at *m/z* 907, 881 and 925, probably corresponding to the pseudomolecular ions $[C_{54}H_{92}O_9$ (linoleate) + $Na]^+$, $[C_{52}H_{90}O_9$ (palmitooleate) + $Na]^+$ and $[C_{55}H_{98}O_9$ (nonadecanoate) + $Na]^+$. Therefore, EM1 was defined as a mixture of various fatty acid M1 mono-esters including stearate, oleate and palmitate. The linkage position of fatty acyl moieties to M1, however, could not be determined because the amount of EM1 isolate was insufficient for ^{13}C-NMR analysis.

Regarding the position of fatty acyl moiety connected to M1, the 3β-hydroxy group of aglycone moiety is believed to be esterified with fatty acids like cholesterol, by acyl CoA: cholesterol acyltransferase (ACAT). Moreover, fatty acids may be also linked to M1 at C-6 of the glucose moiety as described for the action of acyl CoA: triterpene acyltransferase (ATAT) which differs from ACAT.[13] Detailed analyses to answer this issue are now in progress using MS and NMR.

Enhancement of antitumor activity of M1 by fatty acid esterification[11]

The antitumor activities of M1 and EM1 was examined, using a solitary hepatoma model by intrahepatic implantation of B16-F10 cells in C57BL/6 mice. The growth of implanted tumor tended to be inhibited in mice administered with M1 by 23% (not significant compared to the untreated control) (Fig. 5). In contrast, the treatment of EM1 at the same dosage as M1 caused a significant inhibition of tumor growth compared with either the untreated control ($p<0.002$) or

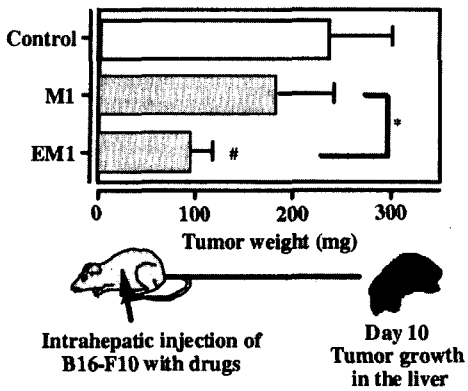

Fig. 5. Effect of M1 and EM1 on the Growth of B16-F10 after Intrahepatic Implantation.
C57BL/6 female mice were anesthetized with pentobarbital (50 mg/kg) and immobilized. A sub-xiphoid transverse incision was then made through the skin, exposing the liver that was externalized and isolated with sterile 2-×2-cm gauze. Using a 29-gauge needle attached to a 0.5 ml insulin syringe, the suspension of tumor cells (1.5×10^7/ml) with or without drug (M1 or EM1) in DMPC liposomes (drug : DMPC, 1:9 mol%) was injected under the liver capsule (12.5 μl, 2×10^5 tumor cells and 5 mg/kg drug/mouse). Liposomes were used as drug matrices because of hematological safety. Mild pressure was applied for 30 s to prevent hemorrhage and tumor extravasation, and the abdomen was then closed in one layer with 9-mm Autoclip-wound clips. The mice were allowed to recover and then returned to their cages. Ten days later, mice were sacrificed and a solitary tumor grown in the liver was weighed. Each column represents the mean±S.D. of 6 animals. #, $p<0.002$ *vs.* control; *$p<0.02$ *vs.* M1-treated group by Student's two-sided *t* test.

M1-treated group ($p<0.02$).

To clarify the relationship between the antitumor efficacy of M1 and EM1 and their tissue concentrations in the liver, the hepatic levels of M1 and EM1 following their i.v. administration were examined. Consistent with our previous finding (Fig. 1A), M1 was selectively taken up into the liver soon after its administration, peaking within 10 min (C_{max}, 65% recovery), and was thereafter cleared rapidly from the liver (Fig. 6). On the other hand, EM1 was also rapidly accumulated in the liver (T_{max}, 40 min; C_{max}, 43% recovery), but the EM1 level decreased gradually with time, and over 25% of the dose (120 μg/g wet tissue) was sustained for 24 h after administration. These results indicate that the antitumor efficacy was dependent on the hepatic accumulation. Since only a small amount of M1 resulting from deacylation of EM1 in the liver was detected, the rate of deacylation of EM1 in the liver appears to be very low. In addition, because EM1 is not excreted as bile as M1 is (Fig. 3), it must be cleared very slowly from the liver and accumulated in the liver for a longer period than M1.

Esterification of M1 with fatty acid resulted in a marked increase of the antitumor potential of M1

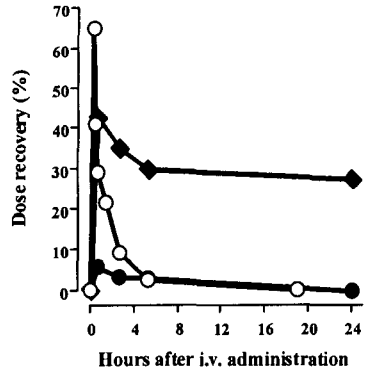

Fig. 6. Time Course of the Hepatic Levels of M1 and EM1 after i.v. Administration.
C57BL/6 mice were given a single i.v. injection of M1 or EM1 at a dose of 30 mg/kg (0.1 ml/20 g body weight). At the indicated time after administration, the dose recovery of M1 and EM1 in the liver was determined by HPLC. Each point represents the mean value of % dose recovery from two to three animals (◆ , EM1; ○ , M1; ● , M1 deacylated from EM1).

(Fig. 5) and that the antitumor activity paralleled with the pharmacokinetic behavior (Fig. 6). So far, improvement of antitumor drugs by fatty acid esterification has been experimentally attempted with the aim of increasing the cellular uptake of the drugs and delaying their metabolic deamination and clearance. Breistφl *et.al.* reported that a fatty acid ester derivative of cytarabine is more effective for the treatment of hematological malignancies than cytarabine.[14] Thus, the enhanced antitumor effect of EM1 may be closely associated with its persistent retention in the liver.

The effects of EM1 and M1 on the growth of B16-F10 melanoma cells *in vitro* were examined using Tween 20 (Tw) or dimyristoylphosphatidylcholine (DMPC) as drug matrices. Although EM1 as well as M1 inhibited tumor growth in a dose-dependent manner, EM1 was the less cytotoxic of the two (Fig. 7).

An issue raised here is which active principle, M1 or EM1, is required for expression of the antitumor effects of ginsenoside. The dammaranediol in M1 is structurally similar to cholesterol. Although M1 shows relatively selective cytotoxicity against tumor cells compared with normal cells *in vitro*,[15] excessive intracellular M1 may become toxic to normal cells. Because EM1 was less cytotoxic than M1 *in vitro*(Fig. 7), the esterification of M1 may represent a detoxification reaction, just as cholesterol esterification is shown to prevent the cytotoxicity of excess intracellular cholesterol.[16] It is also possible that the effect of EM1 may not depend on itself but the resultant M1 from deacylation of EM1 by esterase. Neither M1 nor cholesterol oleate stimulated splenic lymphocytes to become cytotoxic to tumor cells, whereas EM1 promoted the tumor cell

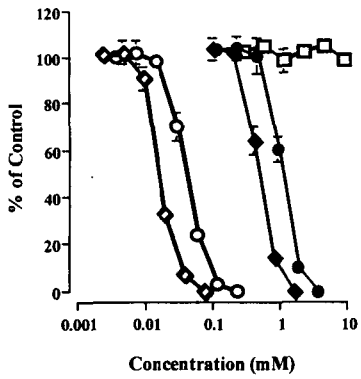

Fig. 7. *In vitro* Cytotoxicity of M1 and EM1 against B16-F10 cells.
B16-F10 cells (2×10^5/well) were seeded into 96-well plates and cultured in growth medium with or without serial 1:2 dilutions of drugs. One day after incubation, the cell number was counted using the trypan blue dye exclusion method. Each point represents the mean±S.D. of three dishes (◇ , M1-Tw; ○ , EM1-Tw; ◆ , M1-DMPC; ● , EM1-DMPC; □ , DMPC alone).

lysis mediated by lymphocytes, particularly non-adherent splenocytes, in a concentration-dependent manner (data not shown).[11] These results clearly indicate that EM1 can induce host-mediated responses more strongly that M1. Therefore, if the esterification of M1 is a detoxification reaction, the resultant esters (*i.e.* EM1) can potentiate M1 through efficient accumulation.

Biotransformation of M1 to 3-O-oleoyl M4

Biodistribution and metabolism of M4[12]

For pharmacokinetic analysis of M4, the mice administered orally with M4 for 30 days were sacrificed, and the contents of gastrointestinal tract and the digestive organs (biological samples) were analyzed in detail by TLC and HPLC.

The typical TLC profiles are summarized in Fig. 8. As shown in Fig. 8B, M4 was detected in the diet dosed with M4 (lane 1+), the stomach (lane 2+), the large intestine (lane 4+), the feces (lane 5+) and the mesenteric lymph tissues (lane 7+), whereas it was not detected in either the small intestine (lane 3+), the blood (lane 6+), the liver (lane 8+) or the lung (lane 9+). Based on the comparison of biological samples between the M4-treated and untreated animals using various solvent systems, the new band at the *Rf* value of 0.44 (termed as EM4) was found to exist in the small intestine (lane 3+), the mesenteric lymph tissues (lane 7+, though the band was twist), the liver (lane 8+) and the lung (lane 9+), but not in the blood (lane 6+). Although the band of EM4 appears to exist in the diet dosed with M4 (lane 1+), precise TLC analyses have denied such

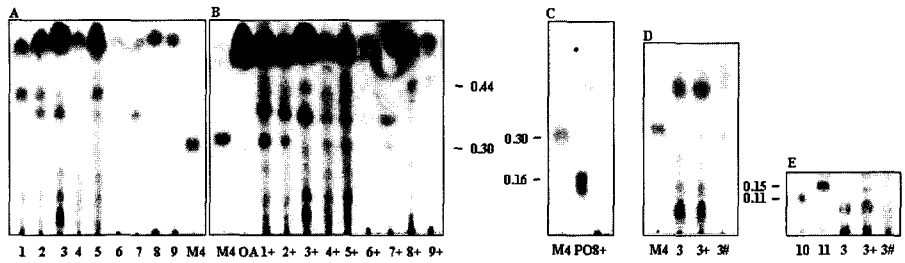

Tissue sample No.:	1	2	3	4	5	6	7	8	9	1+	2+	3+	4+	5+	6+	7+	8+	9+
Net weight (g wet)	1.82	1.70	3.50	2.34	1.32	3.51	2.64	4.32	0.70	1.93	1.49	3.32	2.68	1.56	2.43	2.37	4.44	0.76
AcOEt extract (mg)	42.6	28.3	92.7	19.6	35.6	3.97	545	115	20.3	91.1	36.2	270	40.2	45.2	9.39	567	101	34.0

Fig. 8. TLC Profiles of Distribution and Metabolism of M4 in the Gastrointestinal Tract and Digestive Organs after Its Oral Administration.

C57BL/6 mice were given the diet dosed with or without 0.05% M4 (73 mg/kg/d). The animals were sacrificed day 30 after tumor implantation, and the contents of gastrointestinal tract and the digestive organs were extracted with AcOEt. The weights of tissues (g wet) and their AcOEt extract (mg) are summarized in the table at the foot of the figure. The AcOEt extracts (tissue samples) were analyzed by TLC [TLC plate, silica gel 70 F_{254}; developing solvent, $CHCl_3$-EtOH (10 : 1 v/v) (**A**, **B** and **D**), AcOEt (**C**) or $CHCl_3$-EtOH (50 : 1 v/v) (**E**); plate **A**, TLC data from control animals (lane 1, diet; lane 2, stomach; lane 3, small intestine; lane 4, large intestine; lane 5, feces; lane 6, blood; lane 7, mesenteric lymph tissues; lane 8, liver; lane 9, lung; lane M4, M4); plate **B**, TLC data from M4-treated mice (each lane +, the same tissue samples as plate **A**; lane OA, oleic acid); plate **C**, TLC data from comparison of the liver sample from M4-treated mice with M4 or PO; plate **D**, TLC data from comparison of alkaline hydrolysate (lane 3#) with its normal samples (lanes 3 and 3+); plate **E**, TLC data from comparison of EM4 with chemically (lane 10) or enzymically (lane 11) synthesized M4 oleate].

possibility (data not shown). Furthermore, EM4 did not result from *ex vivo* incubation of M4 in the contents of small intestine from untreated mouse (data not shown). These results suggest that orally administered M4 is completely absorbed from the small intestine and transferred mainly into the mesenteric lymphatics followed by formation of EM4 and its spreading to other organs in the body and excretion as bile. When M4 was injected into the tail vein of mice, it was undetectable in the blood or liver even after 3 min of administration (data not shown), so the metabolic reaction seems to progress quickly in the body. M4 appeared again in the large intestine (Fig. 8B, lane 4+), suggesting the deacylation of EM4 by colonic bacteria.

Alkaline treatment of the contents of small intestine from M4-administered mice resulted in M4 (Fig. 8D, lane 3#), indicating that EM4 is ester. Because oleic acid (OA) was rich in the diet and all the tissues tested (Fig. 8B), the oleic acid esters of M4 were synthesized and compared with EM4. On a TLC plate, the *Rf* value of EM4 was consistent with that of the enzymically synthesized M4 oleate (11) (Fig. 8E, lanes 11 and 3+).

Structural Elucidation of EM4

HPLC analysis showed the same t_R value of 24.5 min between EM4 and **11**. Therefore, EM4 was considered identical to **11**; however, EM4 was not isolated in sufficient amounts to be analyzed for MS and NMR. The linkage position and number of oleic acid(s) to M4 in EM4 were determined using **11**.

Low resolution FAB-MS of chemically synthesized M4 oleate (**10**) and **11** in the presence of added NaCl produced a same strong ion at *m/z* 763 corresponding to the pseudomolecular ion $[C_{48}H_{84}O_5+Na]^+$. Furthermore, high resolution FAB-MS gave ions at *m/z* 763.6248 ($C_{48}H_{84}O_5Na$, $[M + Na]^+$; theoretical *m/z* 763.6217) for **10** and 763.6202 ($C_{48}H_{84}O_5Na$, $[M + Na]^+$; theoretical *m/z* 763.6216) for **11**. These data indicate that both 2 esters are mono-esters of M4 with oleic acid. In the ^{13}C- and ^1H-NMR spectra of **10** and **11**, carbon and proton signals were assigned by ^1H-^1H shift correlation spectroscopy (COSY), heteronuclear multiple-quantum correlation (HMQC) and heteronuclear multiple-bond correlation (HMBC) measurements. Although the C-6 and C-20 carbon signals remain almost unchanged, the C-3 and C-12 carbon ones differ between the two (Table 1). Such differences are also observed in the ^1H-NMR spectrum. The downfield

Table 1. ^{13}C-, ^1H-NMR Data of Hydroxy Carbons and Protons Involved in the Oleoyl Derivatives of M4[a)]

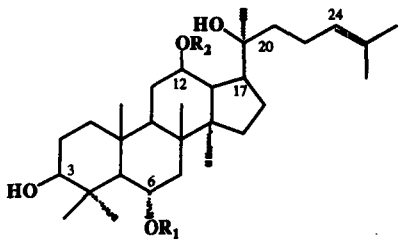

10: R_1 = oleoyl, R_2 = H **11**: R_1 = H, R_2 = oleoyl

	10	**11**
Carbons:		
C-3	76.8	80.1
C-6	66.2	66.0
C-12	73.4	69.7
C-20	72.3	72.0
Protons:		
H-3	2.92 (dd-like)	4.33 (dd, J = 11.2, 5.1)
H-6	3.89 (m)	3.89 (td-like)
H-12	4.75 (td, J = 10.4, 5.3)	3.40 (td-like)

a) Measured in DMSO-d_6 at 400 MHz. Chemical shifts are in δ (ppm) and J values are in Hz.

shifts of C-12 carbon and H-12 proton signals in **10** or C-3 carbon and H-3 proton signals in **11** show that **10** is 12-*O*-oleoyl M4 and **11** is 3-*O*-oleoyl M4. Therefore, the metabolic reaction of M4 in the body may be catalyzed by the enzyme with similar mechanical properties to the microbial lipase MY30 produced by *Candida cylindracea*.[17]

Although Kasai *et al.* have reported that the oxidation of M4 by a rat liver microsomal fraction affords its 24,25-epoxide (PO),[18] this compound was undetectable in the liver from M4-treated mice (Fig. 8C, Lane 8+). In addition, the glucuronide of M4 was not also detected (data not shown), as such glycosides as glycyrrhetic acid and baicalein, the sapogenins of glycyrrhizin and baicalin, are conjugated with glucronic acid.[19] Therefore, metabolic regulation of M4 may differ from the detoxification catalyzed by liver microsomal cytochrome P450.

M4 was esterified with fatty acid as M1 is (Fig. 3). M4 is structurally similar to cholesterol; so M4 may enter the same metabolic pathway as cholesterol. This concept may be partly supported by the *in vitro* study by Kwon *et al.* of the inhibitory activity of M4 against acyl CoA: cholesterol acyltransferase (ACAT).[20] The selective accumulation of M1 in the liver was not observed with respect to M4. M1 chemically consists of dammaranediol and glucose. Hepatocytes can recognize glucose moiety *via* a receptor except for galactose receptor.[21, 22] Therefore, this specific function of hepatocytes must be partly associated with the selective accumulation of M1 into the liver.

Metabolic regulation of M1 and M4 in the tissues differed from those glycosides which are conjugated with glucronic acid (*ex.* glycyrrhetic acid and baicalein, the sapogenins of glycyrrhizin and baicalin).[19] To our knowledge, there have been few reports on animal fatty acid triterpene esters, except for two reports by Tabas *et al.* who isolated the triterpene esters containing 80% stearate and 20% palmitate from the liver of rabbits and humans.[23] They hypothesized that the origin of fatty acid triterpene esters may be *via* dietary absorption of plant triterpenes followed by fatty acid esterification of the triterpene in animal tissues.[13] The detection of fatty acid mono esters of M1 and M4 in the tissues is the first evidence for their hypothesis.

Enhancement of immunostimulating activity of M4 by fatty acid esterification

The oral administration of M4 at doses (3-13 mg/kg/d) prior to tumor implantation also prevented the growth of B16-BL6 melanoma at the implanted site in both male and female mice (data not shown).[12] This suggested that M4 induced host-mediated responses required to inhibit tumor growth. Such responses are involved in immune cells. NK cells destruct tumor cells by

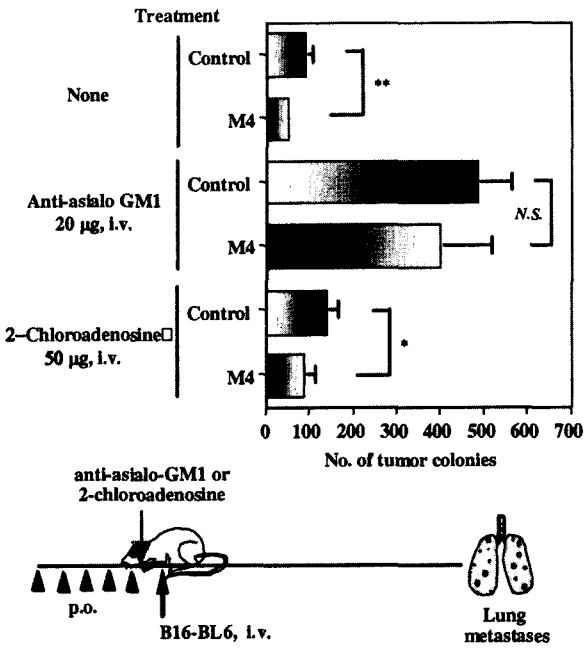

Fig. 9. Antimetastatic Effects by Oral administration of M1 or M4 before Tumor Inoculation.
Female C57BL/6 mice were administered orally with or without M1 or M4 for 5 days (5 mg/kg/day) before an i.v. injection of B16-BL6 cells (3×10^4 cells/mouse). Anti-asialo GM1 serum or 2-chloroadenosine was administered i.v. at 24 h before tumor inoculation (*i.e.* immediately after the last administration of M1). After 14 days of tumor inoculation, the animals were sacrificed and the number of tumor colonies in the lung was counted manually. The results represent the mean±S.D. of 6 mice per group. *, $p<0.05$; **, $p<0.01$ *vs.* control by Students two-sided *t*-test. *N.S.*, not statistically significant.

injecting perforin into target cells,[24] and macrophages kill tumors through activation of T cells.[25] Anti-asialo GM1 serum and 2-chloroadenosine can selectively eliminate NK cells and macrophages, respectively.[26] In the lung metastasis produced by i.v. implantation of B16-BL6 cells, the treatment with anti-asialo GM1 serum or 2-chloroadenosine before tumor implantation increased the number of tumor metastatic colonies in the lung by 5 fold or 1.5 fold, respectively, compared with the control group (Fig. 9). In this metastasis model, NK cells seem to play more important roles in preventing metastatic spread of tumor cells than macrophages. The oral administration of M4 prior to tumor implantation significantly abrogated the enhanced metastasis in the mice pretreated with 2-chloroadenosine (*i.e.* macrophage-eliminated mice), but not in the mice pretreated with anti-asialo GM1 serum (*i.e.* NK cell-eliminated mice) (Fig. 9). Therefore, the antimetastatic mechanism of M4 was principally associated with the activation of NK cells.

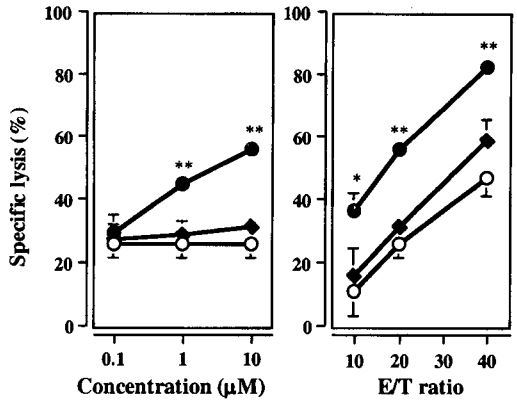

Fig. 10. Effects of M4 and **11** (EM4) on Splenic NK Activity.
Splenocytes ($1\text{-}3\times10^6$/well) and YAC-1 cells (1×10^5/well) were co-cultured with or without M4 or **11** (0.1-10 μM). After 40 h of culture, the number of viable tumor cells was determined by visual inspection. The ability of lymphocytes to lyse tumor cells was calculated as described in the section of Materials and Methods. Each point represents the mean±SEM of 3 dishes (○ , untreated; ● , **11**-treated; ◆ , M4-treated). Left graph, variation of concentrations from 0.1 μM to 10 μM of drug at the E/T ratio of 20; Right graph, variation of E/T ratios from 10 to 40 at the drug concentration of 10 μM. *, $p<0.01$; **, $p<0.001$ *vs.* control by Student's two-sided *t*-test.

Consistent with the case of M1 (Fig. 7), the cytotoxicity of M4 against splenocytes and B16-BL6 was attenuated by its esterification with oleic acid [IC_{50}: 50 μM M4, 109 μM **11** (EM4) for splenocytes; 20 μM M4, 80 μM **11** (EM4) for B16-BL6], whereas the esterification increased the splenic NK activity in concentration- and E/T-ratio dependent manners (Fig. 10). These results clearly indicate that the resultant ester (*i.e.* EM4) stimulates the tumor lysis mediated by NK cells; however, the mechanism of action needs to be examined in detail.

Conclusion

In the latter of the 20th century, pharmaceutical studies on ginseng started in parallel with structural elucidation of ingredients, in order to give scientific grounds to its medical efficacy. Ginseng is administered orally, in general. Therefore, its ingredients must meet gastric juice, digestive and bacterial enzymes in the intestines. Nonetheless, lacking consideration of metabolic behavior, the whole extracts or ingredients have been not a little examined by directly adding to cell cultures *in vitro* or by injecting i.p. or i.v. to experimental animals. Surely, these methods may be useful for intact ingredients but not for their metabolites.

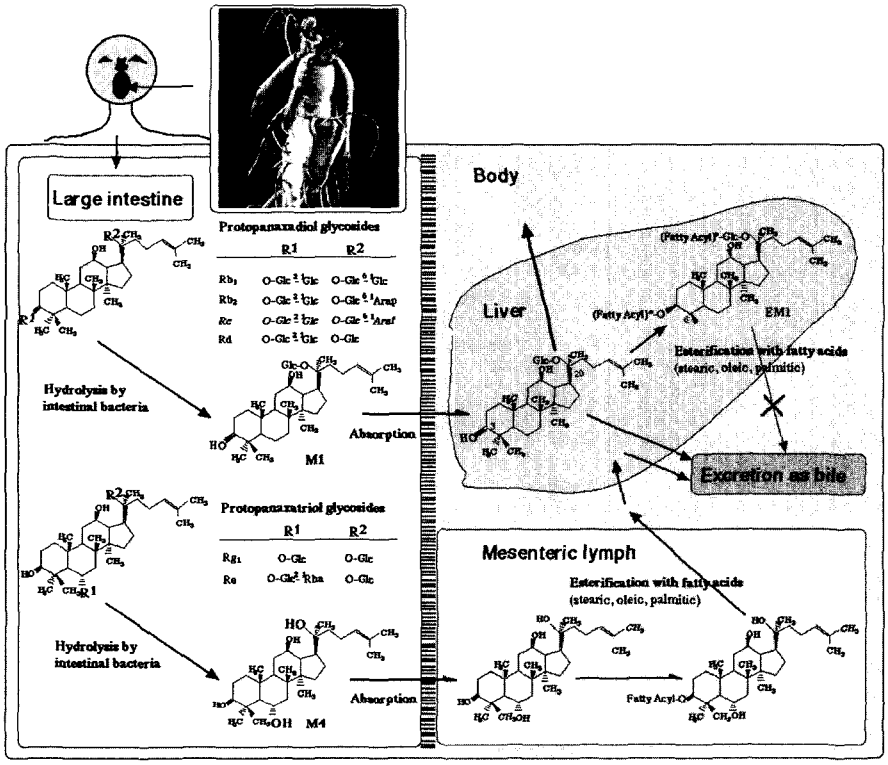

Fig. 11. Possible Metabolic Pathway of Ginsenosides in the Body after Oral Administration.

Our studies using metabolites *in vitro* and *in vivo*, in comparison to parent ginsenosides, have revealed that the anticancer activities of ginseng after oral administration are based on its saponin metabolites formed by intestinal bacterial deglycosylation and hepatic fatty-acid esterification (Fig. 11): The fatty acid esters of metabolite potentiate the antitumor effects through delay of the clearance and through immunostimulation. These findings clearly indicate that the pharmacological studies accompanied by metabolic elucidation of ingredients need to gain a better understanding of the real active principles in the body.

References

1. Hou J. P., *Am. Journ. of Chinese Medicine.* **5**, 123-145 (1977).
2. Tang W., Eisenbrand G., "Chinese Drugs of Plant Origin: Chemistry, Pharmacology, and Use in Traditional and Modern Medicine," Springer Verlag, Berlin, 1992, pp. 711-737.

3. Ng T. B., Yeung H. W., "Scientific Basis of The Therapeutic Effects of Ginseng." In: "Folk Medicine, The Art and The Science," ed. by Steiner R. P., Washington, D.C. American Chemical Society, 1986, pp. 139-151.
4. Shibata S., Tanaka O., Shoji J., Saito H., "Chemistry and Pharmacology of *Panax*." In: "Economic and Medicinal Plant Research," Vol. 1, ed. by Wagner H., Hikino H., Farnsworth N. R., Academic Press, London, 1985, pp. 217-284.
5. Yun T. K., Choi S. Y., *Cancer Epidemiol. Biomarkers Prev.*, **4**, 401-408 (1995).
6. Yun T. K., *Nutrition Rev.*, **54** (II), S71-S81 (1996).
7. Ahn Y. O., *Int. J. Cancer Suppl.*, **10**, 7-9 (1997).
8. Yun T. K., Choi S. Y., *Int. J. Epidemiol.*, **27**, 359-364 (1998).
9. Hasegawa H., *J. Trad. Med.*, **18**, 217-228 (2001).
10. Hasegawa H., Lee K. S., Nagaoka T., Tezuka Y., Uchiyama M., Kadota S., Saiki, I., *Biol. Pharm. Bull.*, **23**, 298-304 (2000).
11. Hasegawa, H., Saiki I., *J. Trad.. Med.* **17**, 186-193 (2000).
12. Hasegawa, H., Suzuki, R., Nagaoka, T., Tezuka, Y., Kadota, S., Saiki, I., *Biol. Pharm. Bull.* **25**, 861-866 (2002).
13. Tabas I., Beatini N., Chen L. L., Su W. C., Puar M. S., Dugar S., Clader J. W., *J. Lipid Res.*, **32**, 1689-1698 (1991).
14. Breistϕl, K., Balzarini, J., Sandvold, M. L., Myhren, F., Martinsen, M., Clercq, E. D., Fodstad, Φ., *Cancer Res.*, **59**, 2944-2949 (1999).
15. Wakabayashi, C., Hasegawa, H., Murata, J., Saiki, I., *Oncol. Res.* **9**, 411-417 (1997).
16. Spector, A. S., Mathur, S. N., Kaduce T. L., *Prog. Lipid Res.* **18**, 31-53 (1975).
17. Myojo K., Matsufune Y., *Yukagaku*, **44**, 183-196 (1995).
18. Kasai R., Hara K., Dokan R., Suzuki, N., Mizutare T., *Chem. Pharm. Bull.*, **48**, 1226-1227 (2000).
19. Kobashi, K., Akao, T., *Bioscience Microflora*, **16**, 1-7 (1997).
20. Kwon B. M., Kim M. K., Baek N. I., Kim D. S., Park J. D., Kim Y. K., Lee H. K., Kim S. I., *Bioorg. Med. Chem. Lett.*, **9**, 1375-1378 (1999).
21. Kawaguchi, K., Kuhlenschmidt, M., Roseman, S., Lee, Y. C., *J. Biol. Chem.* **256**, 2230-2234 (1981).
22. Shimizu, K., Maitani, Y., Takahashi, N., Takayama, K., Nagai, T., *Biol. Pharm. Bull.* **21**, 818-822 (1998).

23. Tabas, I., Chen, L. L., Clader, J. W., McPhail,A. T., Burnett, D. A., Bartner, P., Das, P. R., Pramanik, B. N., Puar, M. S., Feinmark, S. J., Zipkin, R. E., Boykow, G., Vita, G., Tall, A. R., *J. Biol. Chem.*, **265**, 8042-8051 (1990).
24. Oya, H., Kawamura, T., Shimizu, T., Bannai, M., Kawamura, H., Minagawa, M., Watanabe, H., Hatakeyama, K., Abo, T., *Clin. Exp. Immunol.*, **121**, 384-390 (2000).
25. Russo, V., Tanzarella, S., Dalerba, P., Rigatti, D., Rovere, P., Villa, A., Bordignon, C., Traversari, C., *Proc. Natl. Acad. Sci. USA*, **97**, 2185-2190 (2000).
26. Schultz R. M., Tang J. C., DeLong D. C., Ades E. W., Altom M. G., *Cancer Res.*, **46**, 5624-5628 (1986).